

# MD simulation of the WW-loop

This paper summarizes some results of the investigation of energy flow in the WW-loop using MD simulations. The target system is the modified WW loop with 34 residues, where residuum 19 was substituted with azulenylalanine (AZU) and residue 8 was substituted with azidohomoalanine (AHA). AZU can in experiment be excited at a typical wavelength of 600 nm and decays on the sub-picosecond timescale due to internal conversion. Because of this it is well suited to pump energy into the system. AHA has a typical vibrational band at  $2100\text{ cm}^{-1}$  which is separable in the IR spectrum. The AHA-AZU pair is thus well suited for pump-probe-spectroscopy of vibrational energy transport in the WW-loop [1].

The goal of the herein evaluated simulations was to model the heating of AHA and observe the vibrational energy transport through the protein. The simulation flow is the following: All simulations are performed with the GROMACS program suite [2]. and the AMBER99sb\*-ildn force field is used to model the WW-loop and the TIP3P water.

To couple the system to the heat bath, we use the velocity-rescale algorithm [3], and for pressure coupling the Berendsen algorithm[4]. In the beginning the protein was inserted in a dodecahedron box. For the simulation in solvent we add about 1600 water molecules. For the hydrated system we use the Particle-Mesh Ewald method[5] for the electrostatic interactions beyond a miniamal cut-off of 1.4 nm and for the van der Waals interaction a plain cut off at 1.4 nm. After energy minimization, the system is equilibrated for 100 ns at a pressure of 1 atm and a temperature of 100 K. From the second half of this simulation we obtained the average box size for the followed NVT simulation.

We then take 200 statistically independent conformations from a 100 ns 100 K NVT simulation as starting structures for the non-equilibrium simulations. All the starting structures were cooled down to 10 K using a NPT ensemble to improve the signal to noise ratio of the following nonequilibrium simulation.

For the excitation with T-jump method we first freeze out all degrees of freedom of the system except for the chromophore of residue AZU 19. The chromophore is then coupled to a 910 K bath and heated for 1 ps. Following the heating step the velocities of the frozen atoms are set back to the velocities of the corresponding equilibrium step.

Finally the non-equilibrium simulations of all 200 structures were run in a NVE ensemble for 100 ps each, using a timestep of 0.2 fs. The time evolution of the kinetic energy of all residues was averaged over all 200 trajectories and is shown in the plots below.

## 0.1 Results in total kinetic energi

## 0.2 Results in kinetic energy per dof

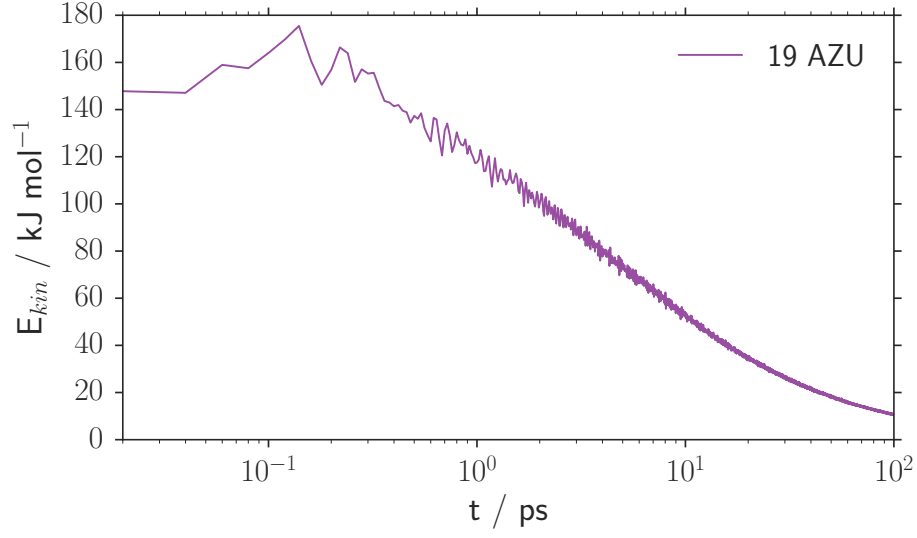


Figure 1: Kinetic energy of the heated residuum AZU 19. The characteristic time of decay between 0.2 ps and 40 ps obtained from fitting is  $\tau_{AZU} \approx 10$  ps.

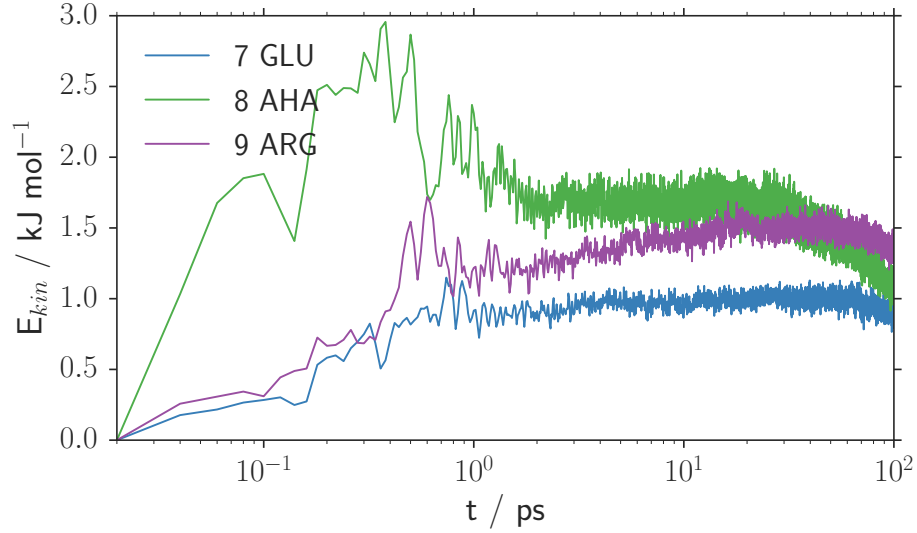


Figure 2: Kinetic energy of residues 7 GLU, 9 ARG and the possible thermometer 8 AHA. The maximum rise in the kinetic energy of 8 AHA is around three times smaller than that of the direct neighbour of AZU 18 TYR. The energies are normalized to the value at  $t = 0$ .

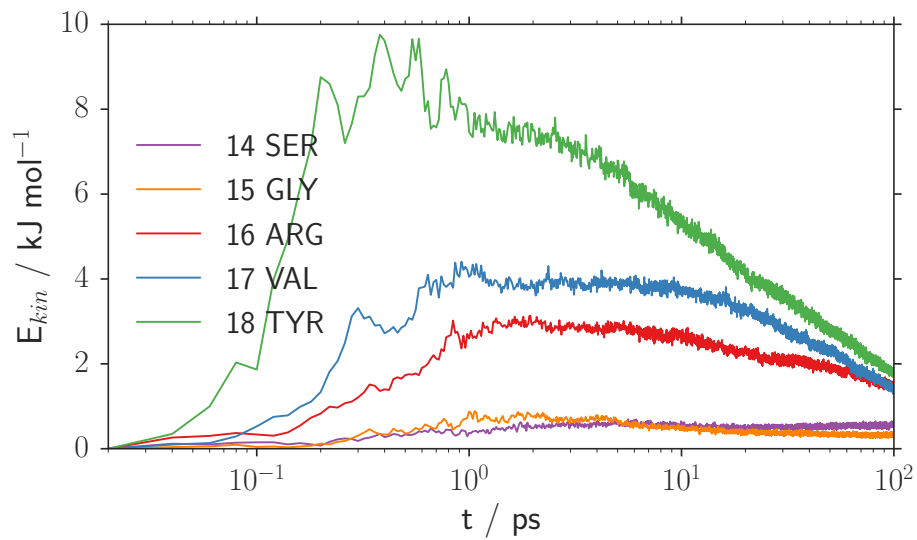


Figure 3: Kinetic energy of downstream residues 14 to 18. The energies are normalized to the value at  $t = 0$ .

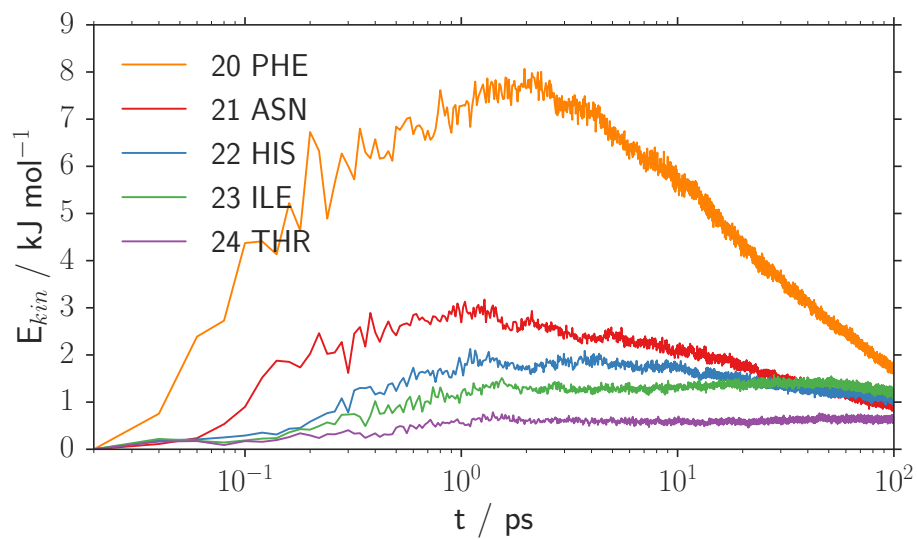


Figure 4: Kinetic energy of upstream residues 20 to 24. The energies are normalized to the value at  $t = 0$ .

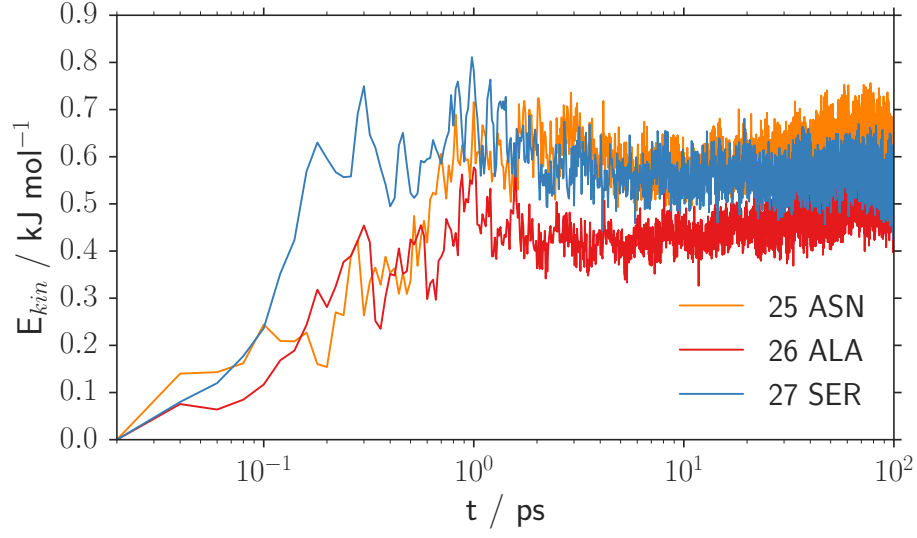


Figure 5: Kinetic energy of residues 25 ASN, 26 ALA and 27 SER. The energy dose for 26 ALA, which is a possible thermometer position, is one order of magnitude smaller than the energy rise of 8 AHA. The energies are normalized to the value at  $t = 0$ .

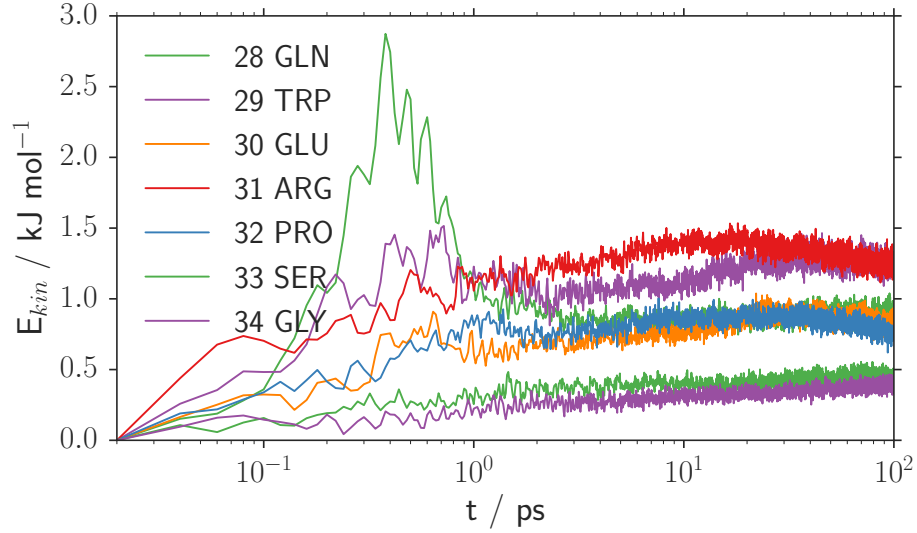


Figure 6: Kinetic energy of residues 28 till end, of which 28 is in polar contact with 19 AZU. The energies are normalized to the value at  $t = 0$ .

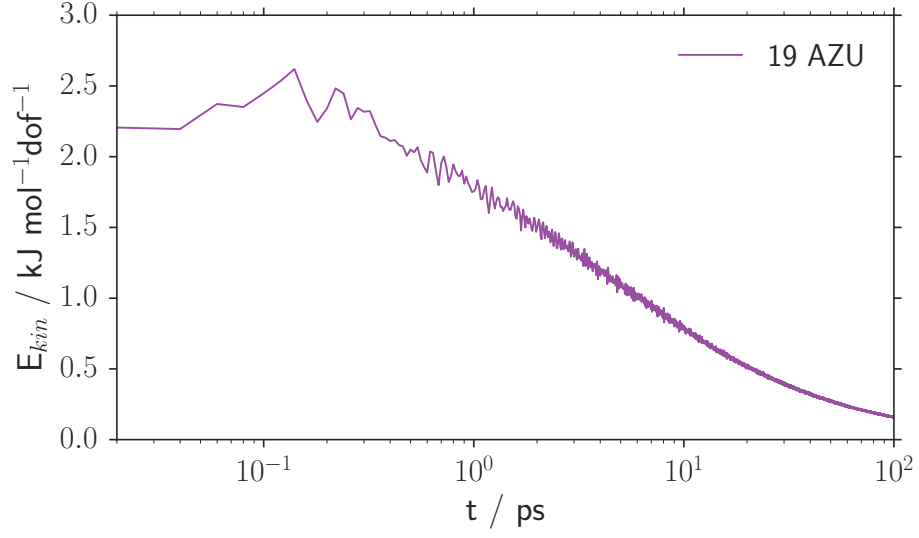


Figure 7: Kinetic energy per dof of the heated residuum AZU 19. The characteristic time of decay between 0.2 ps and 40 ps obtained from fitting is  $\tau_{AZU} \approx 10$  ps.

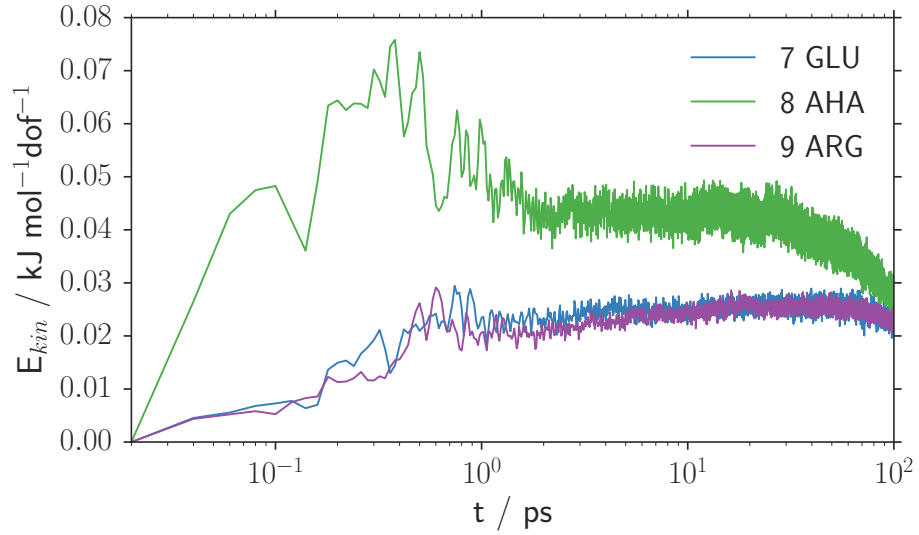


Figure 8: Kinetic energy per dof of residues 7 GLU, 9 ARG and the possible thermometer 8 AHA. The maximum rise in the kinetic energy of 8 AHA is around three times smaller than that of the direct neighbour of AZU 18 TYR. The energies are normalized to the value at  $t = 0$ .

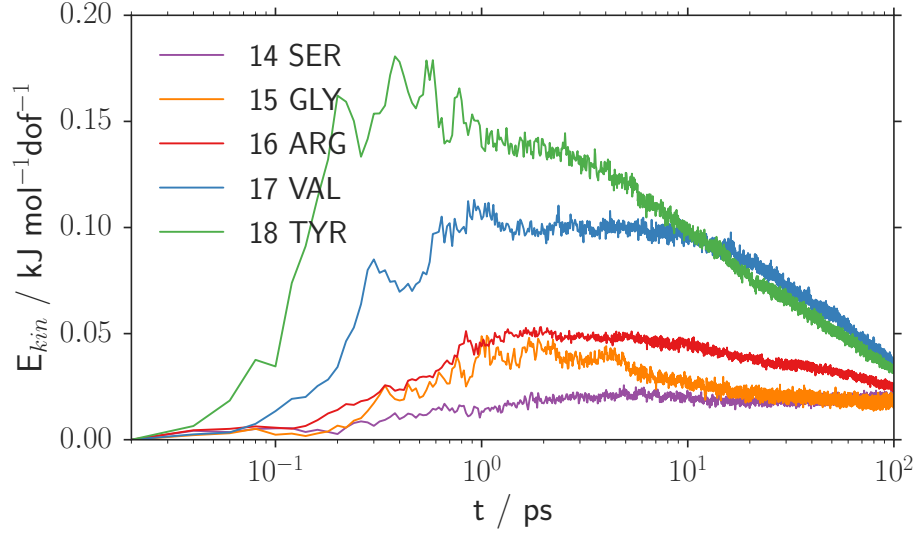


Figure 9: Kinetic energy per dof of downstream residues 14 to 18. The energies are normalized to the value at  $t = 0$ .

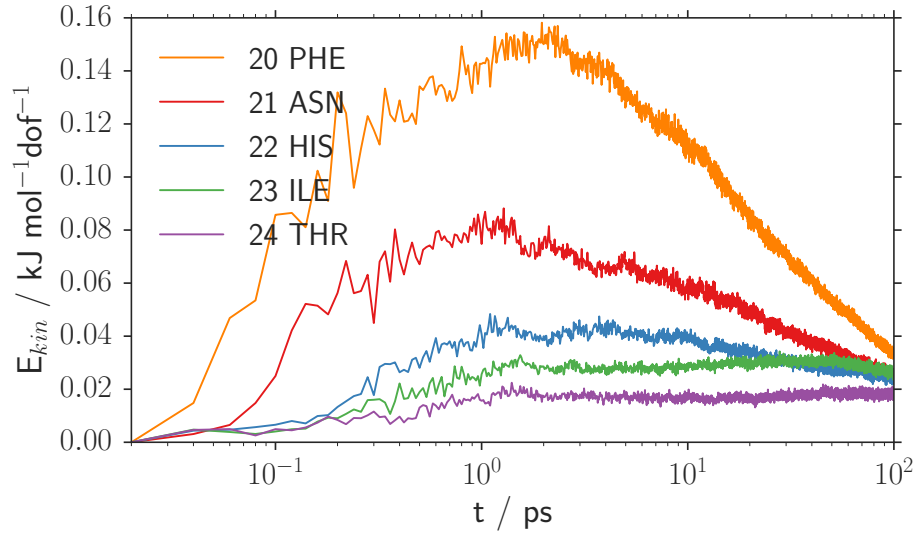


Figure 10: Kinetic energy per dof of upstream residues 20 to 24. The energies are normalized to the value at  $t = 0$ .

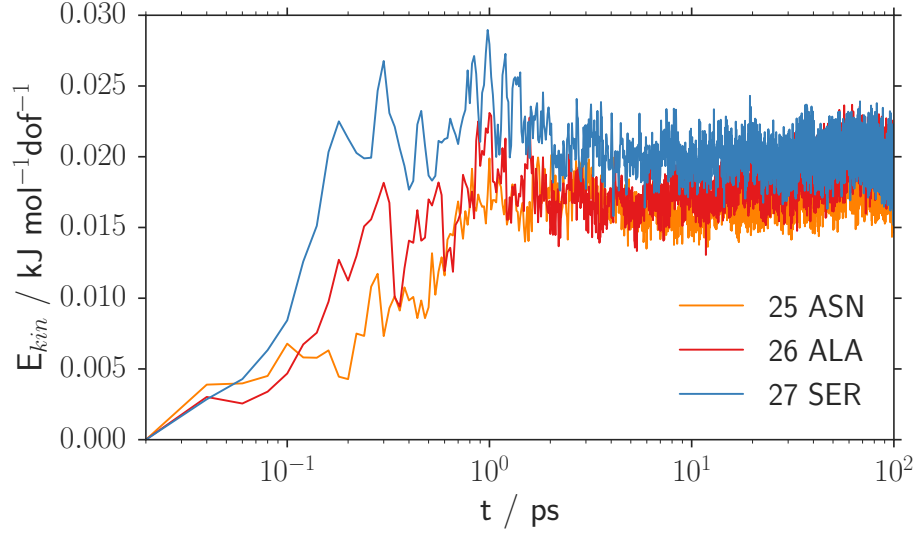


Figure 11: Kinetic energy per dof of residues 25 ASN, 26 ALA and 27 SER. The energy dose for 26 ALA, which is a possible thermometer position, is one order of magnitude smaller than the energy rise of 8 AHA. The energies are normalized to the value at  $t = 0$ .

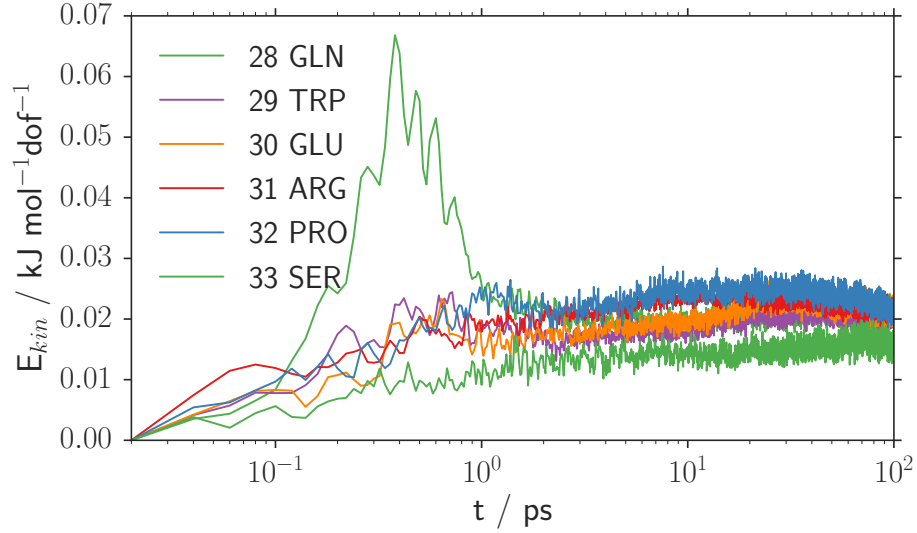


Figure 12: Kinetic energy per dof of residues 28 till end, of which 28 is in polar contact with 19 AZU. The energies are normalized to the value at  $t = 0$ .

# Bibliography

- [1] H. M. Muller-Werkmeister and J. Bredenbeck, A donor-acceptor pair for the real time study of vibrational energy transfer in proteins, *Phys. Chem. Chem. Phys.* **16**, 3261 (2014).
- [2] S. Pronk et al., GROMACS 4.5: a high-throughput and highly parallel open source molecular simulation toolkit, *Bioinformatics* **29**, 845 (2013).
- [3] G. Bussi, D. Donadio, and M. Parrinello, Canonical sampling through velocity rescaling, *J. Chem. Phys.* **126**, 0141011 (2007).
- [4] H. J. C. Berendsen, J. P. M. Postma, W. F. van Gunsteren, A. Dinola, and J. R. Haak, Molecular dynamics with coupling to an external bath, *J. Chem. Phys.* **81**, 3684 (1984).
- [5] T. Darden, D. York, and L. Petersen, Particle mesh Ewald: An  $N \log(N)$  method for Ewald sums in large systems, *J. Chem. Phys.* **98**, 10089 (1993).